A Soft Fabric-based Shrink-to-fit Pneumatic Sleeve for Comfortable Limb Assistance

Richard Suphapol Diteesawat[1], Sam Hoh[1], Emanuele Pulvirenti[1], Nahian Rahman[1]
Leah Morris[2], Ailie Turton[2], Mary Cramp[2], Jonathan Rossiter[1]

***Abstract*— Upper limb impairments and weakness are common post-stroke and with advanced aging. Rigid exoskeletons have been developed as a potential solution, but have had limited impact. In addition to user concerns about safety, their weight and appearance, the rigid attachment and typical anchoring methods can result in skin damage. In this paper, we present a soft, fabric-based pneumatic sleeve, which can shrink from a loose fit to a tight fit in order to anchor to the limbs temporarily, thereby enabling the application of mechanical assistance only when needed. The sleeve is comfortable, ergonomic and can be embedded unobtrusively with clothing. A mathematical model is built to simulate and design sleeves with different geometric parameters. The best sleeve was capable of generating a friction force of 98 N on the limb when inflated to 25 kPa. This sleeve was used to create a wearable assistive device, integrated with a cable-driven actuator. This device was able to lift a 1.44 kg forearm rig up to 95 degree at low pressure of 20 kPa. The device was tested with six healthy participants, in terms of fit, comfort and assistive functionality. The average acceptable sleeve pressure was found to be 33±4.7 kPa. All participants liked the appearance of the sleeve, with a high average perceived assistance score of 7.33±1.6 (out of 10). The shrink-to-fit sleeve is expected to significantly increase the development and adoption of soft robotic assistive devices and emerging powered clothing.**

I. INTRODUCTION

Upper limb weakness is commonly caused by age-related sarcopenia, while limb immobility can occur from trauma, stroke and diseases such as dyskinesia, Parkinsons's, motor neuron disease, and multiple sclerosis [1]. Robotic assistance for upper-limb movement can aid a user to lift and carry loads in daily life, restore body functionality and improve quality of life. Rigid exoskeletons to assist upper limb movement have been widely explored [2]–[5].

Although they provide significant assistance, concerns remain with regard to their safety, weight, ease of use, donning/doffing, and misalignment to the limbs. Soft actuators, in contrast, are commonly light-weight, and offer high force-to-weight ratio and power [6]. Majidi et al. [6] depict the trend of increasing research being conducted on soft and semi-rigid exosuits over the fully rigid exoskeleton in the past two decades. Lightweight soft pneumatic actuators such as pouch motors [7], peano muscles [8], pleated muscles [9], bubble muscles [10], and McKibben muscles [11], [12], are being explored [13] as they are commonly considered more suitable for safe interaction with human body. Assistance using soft actuators has been investigated extensively for rehabilitation and industrial purposes [5], [14]. Although significant advances have been made in actuator technologies, the methods of anchoring them to the human body have not changed much over the years: velcro straps, zippers, stiff garments and rigid components [15]–[19].

As suggested above, one of the major challenges of current exoskeletons is safe and comfortable interfacing with, and anchoring to, the human body. The traditional anchoring methods continuously compress human limbs and can potentially cause damage to skin and muscles including blood flow restriction over long period of use or assistance [15]. Alternatively, active garments were developed for self-fitting capability and ease in donning and doffing by integrating a pneumatic actuator [20] or thermal-responsive shape-changing actuators [21]–[23] into a suit.

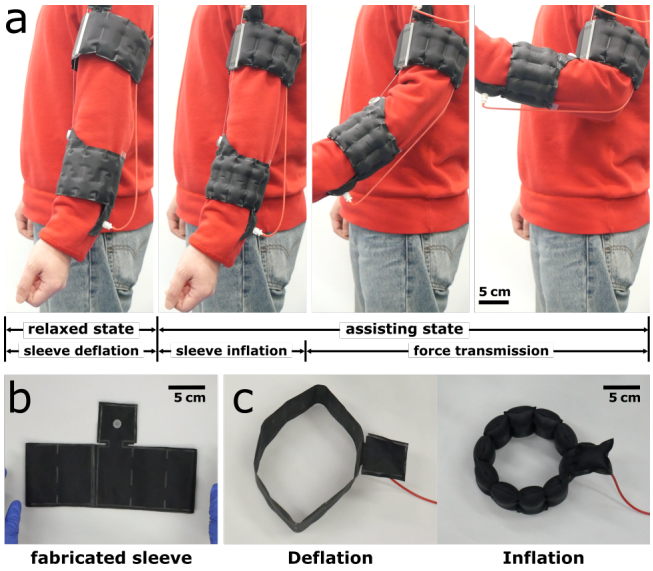

Fig. 1: (a) The wearable device comprising two fabric-based shrink-to-fit pneumatic sleeves and a cable-driven actuator, demonstrating a relaxed state, where the sleeves could be embedded within comfortable clothing, and an assisting state, starting with: i. sleeve inflation, followed by ii. force transmission from the cable-driven actuator to perform arm flexion and finally, iii. sleeve deflation to return to the relaxed state. (b) The fabricated pneumatic sleeve, made of several identical pouch motors, and (c) its deflation and inflation. (Supplementary video is included).

*This work was supported by the Engineering and Physical Sciences Research Council (EPSRC) through grants EP/S026096/1.

[1]RSD, SH, EP, NR and JR are with Department of Engineering Mathematics, University of Bristol, and Bristol Robotics Laboratory (BRL), Bristol, UK richard.diteesawat@bristol.ac.uk

[2]LM, AT and MC are with School of Health and Social Wellbeing, University of the West of England, and BRL, Bristol, UK

In this paper, a novel *shrink-to-fit* pneumatic sleeve (Fig. 1) was developed to overcome this problem and to integrate with soft wearable assistive devices, replacing conventional attachments. The soft shrink-to-fit sleeve can deform itself to fit and anchor on human limbs comfortably. Its dynamic fit, switching between fitting and loosing states, can also be coordinated with assistive actuation such that both tight fit and actuation power are employed together only when required, preventing the issues and concerns mentioned above. The concept and design, mathematical model and fabrication of this pneumatic sleeve are demonstrated in Section II. The experimental setup and results are presented in Section III and IV. The wearable assistive device, human study and conclusions are included in Section IV and V, respectively.

II. Shrink-to-fit Pneumatic Sleeve

A. Concept and Design

The shrink-to-fit pneumatic sleeve was designed by adapting the pouch motor design [7], a simple and lightweight pneumatic actuator, to demonstrate the shrink-to-fit capability. The actuator comprises a series of identical pouch motors connected in parallel to form a hollow cylindrical pneumatic sleeve (Fig. 1b-c). Fabricating from a fabric-based material creates an actuator that resembles normal clothing, remaining soft and flexible when not actuated or pressurized. When inflated, each pouch motor contracts tangentially and expands perpendicularly to the limb surface, causing the entire sleeve to shrink radially, decreasing its internal circumference (Fig. 1c). The pressurised sleeve generates a *compressing* force on the human limb (a normal force on skin). The compression generates a friction force at the skin surface, which counteracts sliding of the sleeve on the limb; this is defined as a *holding* force. Integrating this shrink-to-fit sleeve with an assisting device, such as a cable-driven actuator, enables comfortable, safe attachment on the human limbs and effective force transmission from the assisting device to the body (Fig. 1a).

B. Mathematical model

A mathematical model was built based on the model of pouch motor [7]. The model consists of two main parts: (1) designing a sleeve following set condition and (2) simulating its actuation behaviour.

First, a set of parameters from a human limb and the pneumatic sleeve were selected as initial parameters to design a sleeve: limb diameter (d_{limb}), number of identical pouch motors (n) and their radial length (h), as shown in Fig. 2a. d_{limb} is used to create a circular cross-section of the human limb (assuming a cylindrical limb); n divides this circle into n sectors, each occupied by a single pouch motor. h is the maximal radial length of the actuator at its centre when the actuator just contacts the human limb (defined as set condition). These three parameters were chosen because d_{limb} defines the target limb size and n and h affect the appearance (shape and thickness of the sleeve on the limb) and pressure distribution of the sleeve when contacting the limb. β is the angle between lines separating adjacent sectors, drawn from the centre of the limb, where $\beta = 360°/n$.

We assume that the sleeve is larger than the limb when fully deflated (a necessary condition for wearing), and all identical pouch motors deform uniformly with increasing actuator angle (θ) (Fig. 2b). According to pouch motors [7], θ varies from 0° (an actuator is fully deflated) to 90° (maximum actuator expansion with a circular cross section). Different sleeve designs can have different maximal expansion h when they just touch the limb, and this affects θ at the set condition, $\theta(h)$ (Fig. 2c). Hence, $\theta(h)$ can vary between 0° (h = 0 mm, no space between the uninflated pouch motors and the limb) and some maximum angle $\theta(h) \leq 90°$. β and $2\theta(h)$ can be dissimilar as β is fixed by n, and $\theta(h)$ varies by h as explained above. For example, a given maximal expansion h in Fig. 2b has $2\theta(h)$ less than β.

Providing the set condition (d_{limb}, n and h), the axial actuator length (l) at h, $l(h)$, can first be derived by using equation 1 (Fig. 2a). Then, the actuator angle at this h, $\theta(h)$, and an initial actuator length, l_0, can be calculated from equation 2 (Fig. 2c). The calculated l_0 is always fixed since the sleeve is made of an inextensible material. In addition, l and l_0 are the parameters when considering a cross-section of the sleeve, whereas D is the sleeve width along a limb (Fig. 2a).

$$l(h) = (d_{limb} + h) \cdot \tan(\beta/2) \tag{1}$$

$$\begin{aligned} \theta(h) &= 2 \cdot \tan^{-1}\left(\frac{h}{l(h)}\right) \\ l_0 &= l(h) \cdot \left(\frac{\theta(h)}{\sin\theta(h)}\right) \end{aligned} \tag{2}$$

After acquiring the sleeve design matching set condition, we later use θ and l_0 to simulate its actuation behaviour and shape at different angle ($\theta \leq \theta(h)$). θ defines the actuator shape, which now varies from 0° (fully deflated) to $\theta(h)$ (the sleeve first contacts the limb; set condition). Fig. 2d shows the example of the actuator shape at certain θ less than $\theta(h)$ with non-maximal expansion where the sleeve does not touch the limb. The axial actuator length and contraction at this given θ, $l(\theta)$ and $\varepsilon(\theta)$, can be derived following the model of pouch motor [7] in the following equations. Note that, $l(\theta)$ is equal to $l(h)$ when $\theta = \theta(h)$.

$$l(\theta) = l_0 \cdot \frac{\sin\theta}{\theta} \tag{3}$$

$$\varepsilon(\theta) = \frac{l_0 - l(\theta)}{l_0} = 1 - \frac{\sin\theta}{\theta} \tag{4}$$

The fully-deflated sleeve is simulated as a polygon at θ = 0°; however, the actual sleeve is flexible and will typically form a circle around the limb when relaxed, resembling loose clothing. Thus, the distance between the surface of the limb and the sleeve at full deflation is defined as Δr (Fig. 2b).

The shape of the actuator at any expansion defined by θ (Fig. 2e), can be simulated using $(x(\alpha), y(\alpha))$ by using following equations. When considering the top-most single

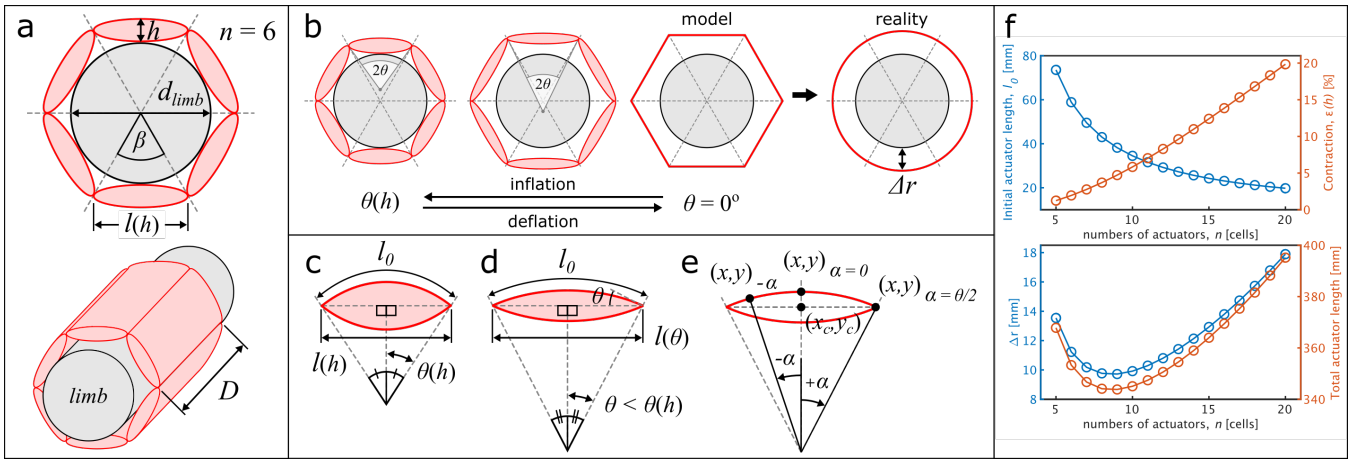

Fig. 2: Schematic diagrams of the shrink-to-fit sleeve consisting of a series of identical pouch motors (e.g. n = 6). (a) The sleeve at set condition, just touching the skin. (b) Actuator shape change from set condition (left) to complete deflation (right). (c-d) The shape of a single pouch motor at (c) set condition, $\theta(h)$, and (d) at an expansion defined by θ. (e) The diagram to simulate an actuator shape. (f) Example of the calculated initial actuator length (l_0), contraction at set condition, $\varepsilon(h)$, displacement between skin and actuator at no actuation (Δr) and total actuator length (l_{total}) of the sleeve made of different numbers of pouch motors, n, at set expansion h of 10 mm, and d_{limb} = 90 mm.

pouch motor (Fig. 2a), the centre of the inflated actuator (x_c, y_c) is at (0, $(d_{limb} + h)/2$), where the centre of the limb is at (0, 0).

$$\begin{aligned} x(\alpha) &= r \cdot \sin(\alpha) \\ y(\alpha) &= r \cdot (\cos(\alpha) - 1) + \frac{h}{2} \\ r &= \frac{l_0}{2\theta} \quad \text{and} \quad \alpha \in [-\theta, \theta] \end{aligned} \tag{5}$$

Because the fabricated wearable device was designed for upper-limb assistance, d_{limb} of 80 mm and 90 mm were selected for a lower arm and an upper arm, respectively. A simulation of the sleeve can be completed from given d_{limb}, n and h. The example for the upper arm is presented in Fig. 2f, illustrating the relationships of l_0, $\varepsilon(h)$, Δr, and total actuator length ($l_{total} = n \times l_0$) to n, when h is fixed at 10 mm. Overall, l_0 decreases while $\varepsilon(h)$ increases with increasing n. Δr and l_0 have the same trend, and large Δr is required for high shrink-to-fit capability.

C. Fabrication

Shrink-to-fit pneumatic sleeves were made of TPU-coated Nylon fabric (Riverseal® 70 LW, Rivertex, UK) and were fabricated by heat sealing the fabric together following actuator designs created using the mathematical model. A heat-sealing machine was built using a CNC machine (Ooznest Limited, UK), which was modified to mount a customised heat-sealing tool on its end effector, using a soldering iron and a soldering station (T0052918099N and T0053434399N, Weller Tools, Germany).

The fabrication began by preparing and placing two layers of identical fabrics on the CNC machine (TPU-coated sides facing). The sleeve design was uploaded to the CNC machine to move the heated soldering iron across the fabrics following the uploaded design. After completing the sealing process, an air connector was added to the fabric for pneumatic connection.

III. Experiments

A. Experimental setup

Two experiment types were set to investigate (1) the compressing force and (2) the holding, explained in section II-A (Fig. 3). All data were acquired by a data acquisition (DAQ) device (USB-6211, National Instruments, USA), and both experiments were operated through MATLAB.

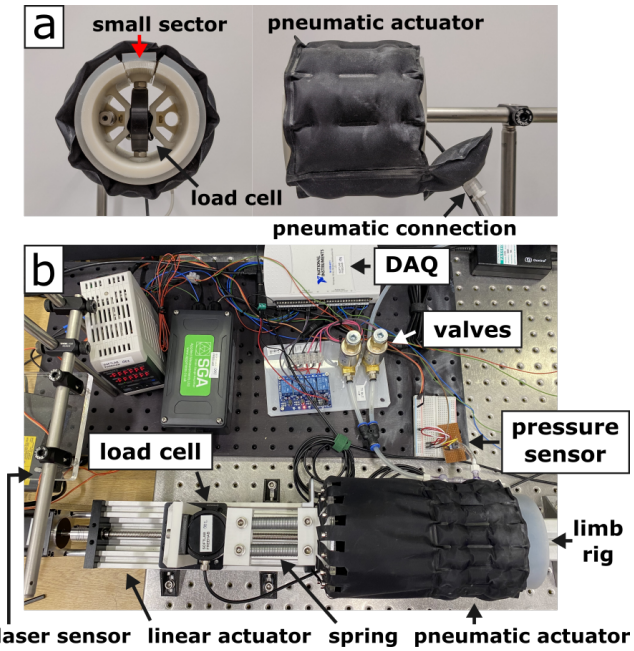

Fig. 3: Experimental setups: (a) compressing force evaluation and (b) holding force evaluation of the shrink-to-fit actuators.

B. Skin compressing force

A human limb equivalent was built with an outer diameter of 90 mm (d_{limb}) to mimic a human arm. It was made of a rigid 3D-printed ABS cylinder with a diameter of 80 mm and wrapped around with a cast 5 mm thick silicone sheet (Ecoflex 00-30, Smooth-On, Inc, USA) to mimic human skin. The cylinder was split into a small sector and a large sector (3(a)) for inserting a load cell (DBCR-100N-002-00, Applied Measurements Ltd., UK) to measure the compressing force exerted by sleeves. The configuration of these dissimilar sectors was intentionally designed to simplify the acquired force data, and the number of pouch motors was even. The measured force is the approximation of the compressing force a single module can generate, and the compressing force from other modules cancel with the ones directly opposite to them as shown in Fig. 3a. Importantly, prior to each experiment, one actuator module of the sleeve was placed at the centre of the small sector.

The shrink-to-fit sleeve was inflated by an air compressor (P100/24 AL, Werther International S.p.A., Germany), and the applied pressure was measured by a pressure sensor (HSCDANN030PGAA5, Honeywell International Inc.).

C. Holding force generation

The same sleeve was then tested to measure its holding force at different pressures (Fig. 3b). A second human limb analogue (d_{limb} = 90 mm) was built for mounting the sleeve and was attached on a rigid bar. One side of the sleeve was clamped and connected to springs, the same load cell and a linear actuator (250 mm C-beam linear actuator, Ooznest, UK) in series. Prior to the testing of each design, the silicone skin was covered in a layer of talcum powder to reduce the intrinsic friction of the silicone and resemble human skin. To begin the experiment, the sleeve was inflated up to a selected pressure, causing it to shrink and compress the limb rig. The sleeve was then pulled by the linear actuator, while the holding force was recorded. The experiment stopped when the sleeve slipped on the rig more than 20 mm, as detected by a laser displacement sensor (LK-G402, Keyence, UK).

IV. Results

A. Shrink-to-fit pneumatic sleeve

Several designs were fabricated to study their actuation behaviour based on two main parameters: number of pouch motors (n) and expansion (h) (Fig. 4). The first set of samples was created by fixing n at 10 cells and varying h at 10, 15, 20, and 25 mm (design D1, D2, D3 and D4), and the second set fixed h at 10 mm and varied n at 6, 10 and 16 cells (design D5, D1 and D6), leading to a total of six samples, where D1 is a member of both sets. The width of all sleeves (D) are set at 80 mm. The compressing and holding forces of these samples on the 90 mm diameter limb rigs are presented in Fig. 5.

Overall, the compressing force of all designs increased with increasing pressure (Fig. 5a); the inflated shape of all sleeves are presented in Fig. 4. Their shape when contacting the limb and the change in sleeve circumference during actuation, considered from the calculated $\varepsilon(h)$ and Δr, vary

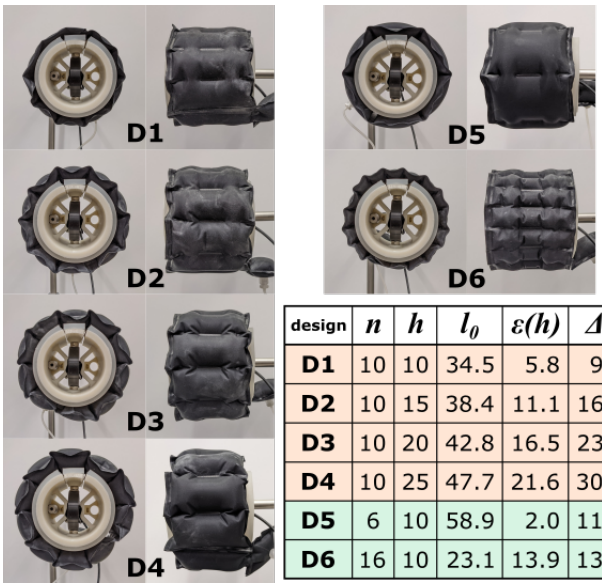

design	n	h	l_0	$\varepsilon(h)$	Δr
D1	10	10	34.5	5.8	9.9
D2	10	15	38.4	11.1	16.1
D3	10	20	42.8	16.5	23.1
D4	10	25	47.7	21.6	30.9
D5	6	10	58.9	2.0	11.2
D6	16	10	23.1	13.9	13.8

Fig. 4: The inflated shape of all sleeve designs (D1 to D6) on the testing limb rig in a front view and a side view. The inset table presents (i) set parameters: n = number of pouch motors (modules), and h = expansion length at set condition [mm], and (ii) calculated parameters: l_0 = initial pouch length [mm], $\varepsilon(h)$ = contraction when the sleeve contacts the limb [%], and Δr = radius difference between full deflation and inflation [mm].

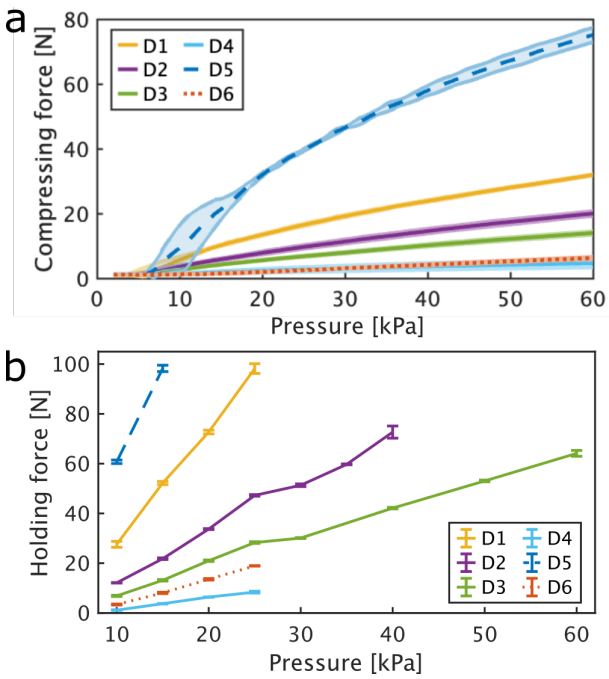

Fig. 5: (a) Compressing force and (b) holding force of six sleeve designs. (a) The sleeves were continuously pressurised from 0 to 60 kPa; shaded areas show one standard deviation. (b) Each sleeve was pressurised at increments of 5 kPa. Values are an average of three trials, and error bars show one standard deviation.

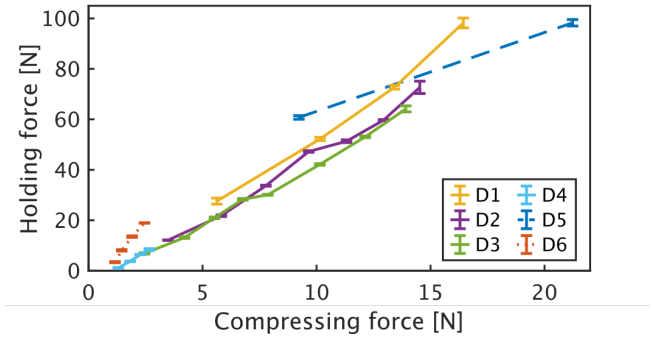

Fig. 6: The relationship between holding force and compressing force of each sleeve design. The holding force and compressing force of each data points are linked by the same pressure obtained from Fig. 5.

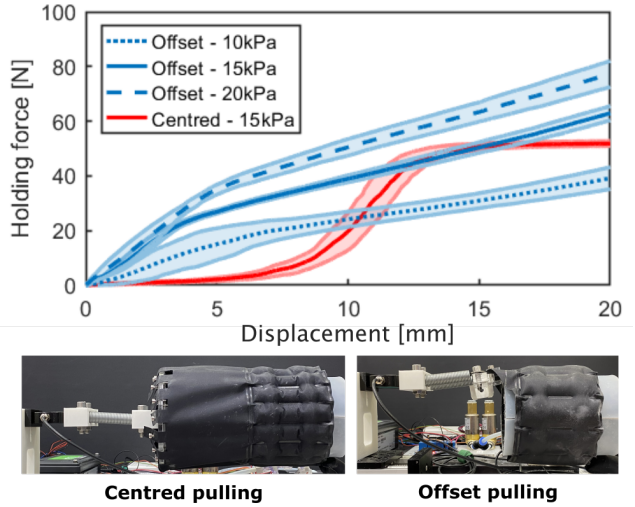

Fig. 7: Holding force with increasing sliding displacement of sleeve design D1 (n = 10 modules, h = 10 mm) at different constant pressures (10, 15 and 20 kPa), acquired from offset pulling experiments. The results of the same design from the centred pulling experiment at 15 kPa are shown for comparison. Insets show 'centred pulling' and 'offset pulling' methods.

across different designs. When n is fixed, sleeves with lower h exerted higher compressing force. h relates to sleeve contraction at set condition, where it initially contacts the skin, $\varepsilon(h)$, corresponding to an actuator expansion shape. With increasing actuation, the pouch motors expand and the surface of the sleeve deforms into a more curved surface. Therefore, for the same n, lower h causes lower $\varepsilon(h)$ (less curved surface when contacting the testing rig; Fig. 4), resulting in larger contacting surface and thus higher compressing force for the same applied pressure. Additionally, as pouch motors can theoretically contract up to 36.34%, the sleeve with low $\varepsilon(h)$ could contract further, exerting tension and higher compressing force.

In contrast, when fixing h and varying n, sleeves with lower n exerted larger compressing force since each pneumatic module has larger length and less $\varepsilon(h)$, leading to larger contacting surface (Fig. 4). In addition, all sleeves started deformation at a low pressure threshold of approximately 5 kPa (Fig. 5(a)). It was observed that the sleeve design D5 (n = 6 modules, h = 10 mm) produced large variation of compressing force at low pressure, ($\leq \sim 10$ kPa). This was because the size of the pneumatic module exceeded the measuring sector.

For holding force evaluation, each sleeve was pressurised at different pressures up to the pressure which produced a compressing force close to 15 N, which we set as the maximum allowable force exerted on human skin. In general, the holding force increased with increasing pressure, and the sleeves with larger compressing force had higher holding force due to higher skin deformation and friction (Fig. 5b).

Figure 6 shows the relationship between the holding force and the compressing force at the tested pressures in the holding force experiments. Sleeve design D1 (n = 10 modules, h = 10 mm) was judged to have performed the best, producing the highest holding force for the same compressing force. Having a higher holding force is important to ensure the sleeve does not slip during actuation, affecting the biomechanics of the delivered assistance. Conversely, a lower compressing force is preferred as it reduces the risk of discomfort and injuries to a user. In addition, Figure 5 shows the sleeve design D1 delivered holding force of 98 N at 25 kPa (equivalent to 16.4 N of compressing force), implying that a low operating pressure can achieve a strong anchor for the subsequent application of mechanical assistance.

The sleeve design D1 was selected as the most suitable design to create a wearable device. It was further investigated by assessing the holding force when pulled from only one side of the sleeve, to mimic a practical usage scenario (Fig. 1a). This experiment is identified as 'offset pulling', whereas the previous experiment is 'centred pulling' (see insets in Fig. 7). The 'offset pulling' experiment represents a specific application for the proposed wearable device, presented in the later section. In contrast, the 'center pulling' experiment was studied as a more general case because the active sleeve can be used in many applications where the goal is to anchor on the body.

Consequently, different patterns of the holding forces between these two different pulling methods were observed. For the 'offset pulling' experiment, the pulled side (top side) started slipping while the opposite side (bottom side) remained in the same position and the holding force kept increasing with measured displacement. During this experiment, the internal pressure of sleeves slightly increased by about 4 to 6 kPa due to the deformation and torsion of the sleeve against the limb.

The experiments were stopped when reaching 20 mm displacement, as an acceptable displacement of soft attachments since large displacement can influence comfort and assistance performance. The maximum holding forces at 20 mm displacement are 39, 63 and 77 N for applied pressure of 10, 15 and 20 kPa, respectively. Compared to the 'centred pulling' experiment at 15 kPa, the sleeve generated higher holding force in the 'offset pulling' experiment.

B. Wearable Assistive Device

A cable-driven actuator was built to provide assistance to the human limbs through shrink-to-fit sleeves (Fig. 8a). It contains three main components: a DC geared motor (321-3164, RS Components, UK) with a torque of 29 Ncm and a speed of 241 rpm, a Nylon cable, and a cable guide tube. The cable was attached to the pulley, mounted on the motor, and passed through the guide tube, of which the other end was fixed on the shrink-to-fit sleeve. Two sleeves were fabricated for the lower arm and upper arm. One sleeve connected to the cable, and the other connected to the cable tube.

An elbow mechanism was built to assess the assisting performance of the wearable device (Fig. 8a). 30 cm long upper arm and 30 cm long forearm linkages (both aluminium) were connected by an aluminium revolute joint, which acted as an elbow joint. Two limb analogues were built and mounted on the lower arm and upper arm linkages with d_{limb} = 80 mm and 90 mm, respectively, to closely resemble human upper limbs.

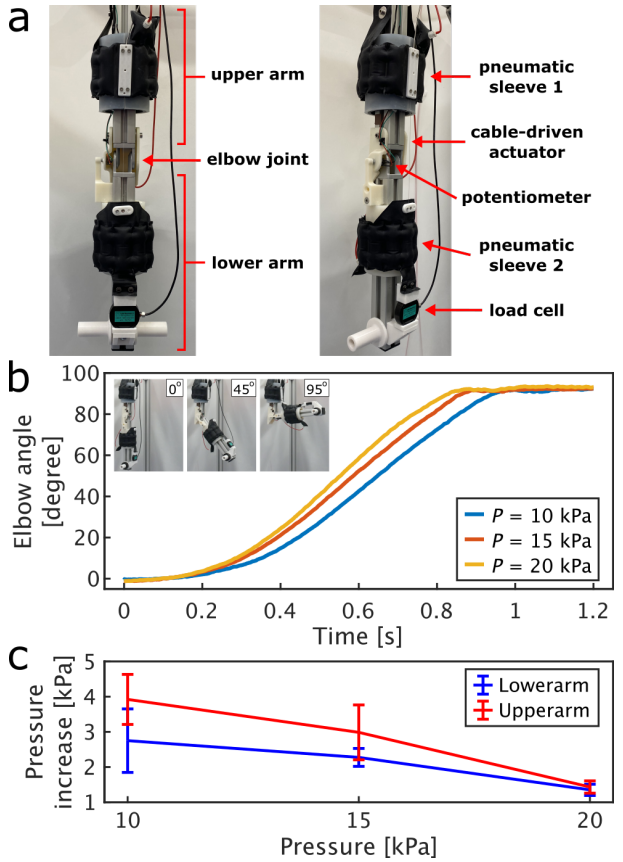

Fig. 8: (a) A wearable assistive device, consisting of a shrink-to-fit pneumatic sleeve and a cable-driven actuator, on a human-like elbow mechanism for assessing the performance of arm flexion. Experiments show (b) average real-time assisted elbow angle at different pressures, and (c) maximum pressure changes of the pneumatic sleeves at different initial pressures (10, 15 and 20 kPa) while performing arm flexion. Three trials were performed for each applied pressure. The maximum angle standard deviation at 10, 15 and 20 kPa were 5.3, 5.5 and 3.5 degrees, respectively.

The wearable device was put on the elbow mechanism and actuated to perform arm flexion as demonstrated in Fig. 8a and Supplementary video. The device was able to lift the lower arm (weight = 1.44 kg) at different pressures (10, 15 and 20 kPa), as illustrated in Fig. 8b. According to [24], the average weight of the lower arm is 0.016 times a body weight. Therefore, the lower arm's weight of this rig is equal to that of a person with the body weight of $\sim$ 90 kg.

The sleeves were disconnected from the air supply system after their internal pressure rose to reach set point, prior to the arm-lifting experiment. During arm flexion, internal pressures increased in the lower arm and upper arm sleeves (Fig. 8c). A higher initial applied pressure caused less pressure increase. The change in pressure happened due to the shape change or compression of the sleeves.

The sliding was assessed by measuring the sliding force from the load cell connected to the sleeve anchored on the lower arm by an additional strip of fabric. Prior to the experiments, this connecting fabric between the sleeve and load cell was loose. After performing arm flexion, the fabric was in tension at low applied pressure (10 kPa) with the maximum measured sliding force of 11.6 N. Referring to Fig. 7, it can be noticed that, at 10 kPa, this force produced a sliding displacement of the sleeve less than 5 mm. For higher pressures, the fabric remained loose after arm flexion. The maximum measured sliding forces decreased with increasing applied pressures: 2.5 N at 15 kPa and 2.6 N at 20 kPa, corresponding to a sliding displacement of less than 2 mm in both cases (Fig. 7). In addition, the speed of arm flexion is higher at 20 kPa. This could be caused by higher rigidity of the inflated sleeves, resulting in higher force transmission and less sliding.

C. Human Study

We invited six healthy participants without upper body impairments to assess our wearable assistive device. Ethical approval for the study was granted by The University of Bristol ethics committee on 31/01/22 (reference 10346). Convenience sampling was utilised to recruit participants from The Bristol Robotics Laboratory. A 14-part written questionnaire was prepared, and the participants were asked to respond to questions regarding actuator appearance, perceived comfort and assistance using an ordinal scale. Four questions allowed the participants to write qualitative responses.

Participants had average lower arm and upper arm diameters of 86.5 mm $\pm$ 0.7 mm and 98.1 mm $\pm$ 0.7 mm, respectively (average value $\pm$ one standard deviation). First, four different designs of the pneumatic actuator (D1, D4, D5, and D6, with varying n and h, see Fig. 4) were tried on their forearm to investigate their preferences in terms of actuator appearance, weight and comfort (1 = unacceptable, 10 = acceptable for its purpose as a comfortable, lightweight assistive device). All designs were inflated at the same pressure of 20 kPa.

The weight scores for all designs were similar, varying between 8 and 10, with an average score of 9.29. The appearance scores for designs D1, D4, D5 and D6 were

8.0±1.4, 7.8±1.5, 7.8±1.5 and 8.0±1.8, respectively. The average comfort score for the sleeve designs D1 and D5 were 7.2±1.2 and 5±1.2, respectively. We do not consider the comfort of the sleeve design D4 and D6 since they did not anchor well on participant's skin (sleeves could slide freely). Participants preferred the designs with smaller actuator pillows (D1 and D6 over D4 and D5) in terms of appearance, but half reported D1 and half reported D6 as their favourite design. Comments regarding the preference for D6 included "Comfort at maximum pressure" (participant 2). Whereas participant 5 preferred D1 and stated that they felt "Design B [D1] was the most comfortable while providing a good hold on my forearm. A and D [D4 and D6] felt like they would slip and move during use."

Later, the participants were then tested with only design D1 to find the sleeve pressure which they found acceptable and safe. The higher the acceptable pressure, the more force transmission and assistance can be provided. The average acceptable pressure across all participants was 33±4.7 kPa. The acceptable pressure for each participant was recorded and was used to actuate the pneumatic components of the shrink-to-fit device, while mechanical power was provided by the cable-driven system. Participants felt that the assistance provided by design D1 was comfortable. However, there were some comments that related to the feeling of pressure and the length of time worn. For instance "It can be worn for long time without pressure. I start to feel it blocking/affecting blood flowing when it is pressured" (participant 1). Similarly, participant 6 stated that comfort was based on short wear, and only speculated whether long wear would be acceptable: "The device (material) is very comfortable and based on the short experiments it won't give any discomfort. Over long time, it should be fine." Participant 3 suggested increased stretch-ability to improve potential discomfort: "My upper arm felt little uncomfortable when lifting weight, if the device has more stretch-ability, it will be more comfortable."

The wearable device was introduced to the participants, and they were instructed on how to use the device for arm flexion assistance. A controller was provided with two buttons for arm flexion and extension; the user was required to press the buttons to perform those motions. On average, they spent 6.8 seconds and 4.1 seconds for donning and doffing the device. The average scores of the ease in donning and doffing were 8.5±1.0 and 9.0±0.6, respectively (1 = very difficult, 10 = very easy). Later, they were required to lift a 500 g weight both without assistance and with assistance. We examined natural assisting motion and level of perceived assistance. Their average scores were 6.7±1.9 (1 = forced motion; 10 = natural motion) and 7.33±1.6 (1 = no assistance, 10 = effective assistance), respectively.

V. Conclusions

In this paper, we present a soft fabric-based shrink-to-fit pneumatic sleeve and its soft anchoring concept as an innovative solution addressing safety concerns and enhancing comfort and durability of wearable assistive devices. We exploit pouch motors as the most current suitable pneumatic actuators to demonstrate this new shrink-to-fit feature. The developed actuator can shrink to different sizes that adapt to different body fits by adjusting the internal pressure of the sleeve. Thereby the actuator can be made to dynamically fit human limbs during pressurisation and subsequent actuation. Traditional medical cuffs cannot achieve this dual function. At no actuation, the sleeve resembles clothing, which is flexible, loose and comfortable to wear and safe for a user. When pressurised, it shrinks to fit firmly and anchor to the upper limbs to effectively transfer assisting forces generated by the cable-driven system to the body. This method also prevents blood flow restriction for long-time wearing.

A mathematical model was developed as a tool to design pneumatic sleeves based on required appearance on human body. Different actuator designs enable the tuning of force output for the same pressure inflation. Hence, several designs were fabricated and characterised regarding their compressing force and holding force. Both generated forces increased with increasing pressure. The desired performance metric was a low compressing force, implying high safety, and a high holding force for effective anchoring and force transmission. The actuator with low contraction when contacting a limb ($\varepsilon(h)$) tends to provide better force outcome at low pressure; however, the shrink-to-fit capability to change its size varies across different designs following the mathematical model.

The sleeve design D1 (n = 10 modules, h = 10 mm) was selected as the most suitable design as it produced a high holding force of 98 N and low compressing force of 16 N on a 90 mm diameter limb at a low operating pressure (25 kPa). This design was subsequently used to create a wearable assisting device integrated with a cable-driven actuator. The device was capable of performing arm flexion on an elbow test rig from 0° to 95° (the maximum angle limit), with a lower arm weight of 1.44 kg, corresponding to that of a 90 kg person. In addition, six participants were recruited to use the proposed wearable device. Although the sample size was small, qualitative findings provide an indication of design acceptability and considerations regarding pressure in respect to length of wear.

Future work will involve the integration of the sleeve into garments and artificial muscles [15], with motion sensors and a control algorithm to create an effective assisting suit to be used in daily activities. This will include the transition from tethered to autonomous onboard air supply. Besides, the shrink-to-fit sleeve can be supplied by recently developed soft non-electromagnetic drivers, e.g. Peano-HASEL [8] and electro-pneumatic pump [25], [26], as potential future solution, replacing conventional heavy, bulky, noisy air pumps and compressors.

As the cross section of the proposed actuator is constant in the axial direction of human arm in this study, increasing the actuator width is expected to increase the force acting on human skin (for the same pneumatic pressure), increasing friction and preventing sliding. Also, wider actuators can generate the same holding force for a lower pressure, which could be more comfortable but would cover more area of the

arm, increasing coverage across tactile mechanoreceptors and reducing breathability. Varying profiles of the pouch, not only a rectangular shape, and exploring other artificial muscles will be conducted to build a more comfortable clothes-like assisting device. Adding a stretchable component as a part of the sleeve can also provide more flexibility when the human arm radially expands during flexion. Combining different pouch designs in one sleeve can tune forces exerting at different parts of the limb for more comfortable anchoring, for example, higher compressing force on hard tissues or bony areas. Further work is needed to balance actuator function, geometry and comfort.

Additionally, the sleeve can be sewn or embedded to normal clothing to fix its anchoring location at the same region to prevent misalignment. Further development of the model to simulate the actuator shape deformation after contacting skin can help predicting accurate force and pressure distribution acting on the skin based on the proposed model simulating actuator shapes. Also, more investigation of the device testing on various arm sizes, non-ideal (non-circular) shapes and better materials closely matching human skin compliance and shear properties, and evaluation of forces exerted from each pouch can improve the knowledge of this technology to create a better device. Last but not the least, future human study will include the measurement of actual force and pressure distribution throughout the skin and blood pressure for physiology monitoring when the device is used.

REFERENCES

[1] A. Roby-Brami, N. Jarrassé, and R. Parry, "Impairment and compensation in dexterous upper-limb function after stroke. from the direct consequences of pyramidal tract lesions to behavioral involvement of both upper-limbs in daily activities," *Frontiers in Human Neuroscience*, p. 336, 2021.

[2] M. A. Gull, S. Bai, and T. Bak, "A review on design of upper limb exoskeletons," *Robotics*, vol. 9, no. 1, p. 16, 2020.

[3] C.-T. Chen, W.-Y. Lien, C.-T. Chen, and Y.-C. Wu, "Implementation of an upper-limb exoskeleton robot driven by pneumatic muscle actuators for rehabilitation," in *Actuators*, vol. 9, no. 4. Multidisciplinary Digital Publishing Institute, 2020, p. 106.

[4] R. Gopura and K. Kiguchi, "Mechanical designs of active upper-limb exoskeleton robots: State-of-the-art and design difficulties," in *2009 IEEE International Conference on Rehabilitation Robotics*. IEEE, 2009, pp. 178–187.

[5] B. Van Ninhuijs, L. Van der Heide, J. Jansen, B. Gysen, D. Van der Pijl, and E. Lomonova, "Overview of actuated arm support systems and their applications," in *Actuators*, vol. 2, no. 4. Multidisciplinary Digital Publishing Institute, 2013, pp. 86–110.

[6] H. Majidi Fard Vatan, S. Nefti-Meziani, S. Davis, Z. Saffari, and H. El-Hussieny, "A review: A comprehensive review of soft and rigid wearable rehabilitation and assistive devices with a focus on the shoulder joint," *Journal of Intelligent & Robotic Systems*, vol. 102, no. 1, pp. 1–24, 2021.

[7] R. Niiyama, D. Rus, and S. Kim, "Pouch motors: Printable/inflatable soft actuators for robotics," in *2014 IEEE International Conference on Robotics and Automation (ICRA)*. IEEE, 2014, pp. 6332–6337.

[8] A. J. Veale, S. Q. Xie, and I. A. Anderson, "Modeling the peano fluidic muscle and the effects of its material properties on its static and dynamic behavior," *Smart Materials and Structures*, vol. 25, no. 6, p. 065014, 2016.

[9] F. Daerden, "Conception and realization of pleated pneumatic artificial muscles and their use as compliant actuation elements," *Vrije Universiteit Brussel, Belgium*, 1999.

[10] R. S. Diteesawat, T. Helps, M. Taghavi, and J. Rossiter, "Characteristic analysis and design optimization of bubble artificial muscles," *Soft robotics*, vol. 8, no. 2, pp. 186–199, 2021.

[11] "Mckibben artificial muscle:," http://cyberneticzoo.com/bionics/1957-artificial-muscle-joseph-laws-mckibben-american/, Accessed 2021.

[12] B. Tondu and P. Lopez, "Modeling and control of mckibben artificial muscle robot actuators," *IEEE control systems Magazine*, vol. 20, no. 2, pp. 15–38, 2000.

[13] T. Abe, S. Koizumi, H. Nabae, G. Endo, K. Suzumori, N. Sato, M. Adachi, and F. Takamizawa, "Fabrication of "18 weave" muscles and their application to soft power support suit for upper limbs using thin mckibben muscle," *IEEE Robotics and Automation Letters*, vol. 4, no. 3, pp. 2532–2538, 2019.

[14] M. Pan, C. Yuan, X. Liang, T. Dong, T. Liu, J. Zhang, J. Zou, H. Yang, and C. Bowen, "Soft actuators and robotic devices for rehabilitation and assistance," *Advanced Intelligent Systems*, p. 2100140, 2021.

[15] V. Sanchez, C. J. Walsh, and R. J. Wood, "Textile technology for soft robotic and autonomous garments," *Advanced Functional Materials*, vol. 31, no. 6, p. 2008278, 2021.

[16] J. Ma, D. Chen, Z. Liu, and M. Wang, "A soft wearable exoskeleton with pneumatic actuator for assisting upper limb," in *2020 IEEE International Conference on Real-time Computing and Robotics (RCAR)*. IEEE, 2020, pp. 99–104.

[17] C. O'Neill, T. Proietti, K. Nuckols, M. E. Clarke, C. J. Hohimer, A. Cloutier, D. J. Lin, and C. J. Walsh, "Inflatable soft wearable robot for reducing therapist fatigue during upper extremity rehabilitation in severe stroke," *IEEE Robotics and Automation Letters*, vol. 5, no. 3, pp. 3899–3906, 2020.

[18] A. Wilkening, H. Stöppler, and O. Ivlev, "Adaptive assistive control of a soft elbow trainer with self-alignment using pneumatic bending joint," in *2015 IEEE International Conference on Rehabilitation Robotics (ICORR)*. IEEE, 2015, pp. 729–734.

[19] T. Abe, S. Koizumi, H. Nabae, G. Endo, and K. Suzumori, "Muscle textile to implement soft suit to shift balancing posture of the body," in *2018 IEEE International Conference on Soft Robotics (RoboSoft)*. IEEE, 2018, pp. 572–578.

[20] T. Helps, M. Taghavi, S. Manns, A. J. Turton, and J. Rossiter, "Easy undressing with soft robotics," in *Annual Conference Towards Autonomous Robotic Systems*. Springer, 2018, pp. 79–90.

[21] B. T. Holschuh and D. J. Newman, "Morphing compression garments for space medicine and extravehicular activity using active materials," *Aerospace medicine and human performance*, vol. 87, no. 2, pp. 84–92, 2016.

[22] R. Granberry, K. Eschen, B. Holschuh, and J. Abel, "Functionally graded knitted actuators with niti-based shape memory alloys for topographically self-fitting wearables," *Advanced materials technologies*, vol. 4, no. 11, p. 1900548, 2019.

[23] L. Tessmer, C. Dunlap, B. Sparrman, S. Kernizan, J. Laucks, and S. Tibbits, "Active textile tailoring," in *ACM SIGGRAPH 2019 Emerging Technologies*, 2019, pp. 1–2.

[24] D. A. Winter, *Biomechanics and motor control of human movement*. John Wiley & Sons, 2009.

[25] R. S. Diteesawat, T. Helps, M. Taghavi, and J. Rossiter, "Electro-pneumatic pumps for soft robotics," *Science robotics*, vol. 6, no. 51, p. eabc3721, 2021.

[26] R. S. Diteesawat, N. Rahman, S. Hoh, and J. Rossiter, "Design exploration of electro-pneumatic pumps (epps) to obtain high pressure and air flow rate improvement," in *Electroactive Polymer Actuators and Devices (EAPAD) XXIV*, vol. 12042. SPIE, 2022, pp. 215–223.